Title

Combination of Immune and Viral Factors Distinguishes Low-Risk versus High-Risk HIV-1 Disease Progression in HLA-B*5701 Subjects

Journal

Journal of Virology, 86(18)

ISSN

0022-538X

Authors

Norström, Melissa M
Buggert, Marcus
Tauriainen, Johanna
et al.

Publication Date

2012-09-15

DOI

10.1128/jvi.01165-12

Peer reviewed

JVI Journals.ASM.org

Combination of Immune and Viral Factors Distinguishes Low-Risk versus High-Risk HIV-1 Disease Progression in HLA-B*5701 Subjects

Melissa M. Norström,[a] Marcus Buggert,[a] Johanna Tauriainen,[a] Wendy Hartogensis,[b] Mattia C. Prosperi,[c] Mark A. Wallet,[c] Frederick M. Hecht,[b] Marco Salemi,[c,d] and Annika C. Karlsson[a]

Department of Laboratory Medicine, Division of Clinical Microbiology, Karolinska Institutet, Stockholm, Sweden[a]; UCSF Positive Health Program, San Francisco General Hospital, University of California, San Francisco, California[b]; and Department of Pathology, Immunology and Laboratory Medicine,[c] Emerging Pathogens Institute,[d] University of Florida, Gainesville, Florida

HLA-B*5701 is the host factor most strongly associated with slow HIV-1 disease progression, although rates can vary within this group. Underlying mechanisms are not fully understood but likely involve both immunological and virological dynamics. The present study investigated HIV-1 *in vivo* evolution and epitope-specific CD8$^+$ T cell responses in six HLA-B*5701 patients who had not received antiretroviral treatment, monitored from early infection for up to 7 years. The subjects were classified as high-risk progressors (HRPs) or low-risk progressors (LRPs) based on baseline CD4$^+$ T cell counts. Dynamics of HIV-1 Gag p24 evolution and multifunctional CD8$^+$ T cell responses were evaluated by high-resolution phylogenetic analysis and polychromatic flow cytometry, respectively. In all subjects, substitutions occurred more frequently in flanking regions than in HLA-B*5701-restricted epitopes. In LRPs, p24 sequence diversity was significantly lower; sequences exhibited a higher degree of homoplasy and more constrained mutational patterns than HRPs. The HIV-1 intrahost evolutionary rate was also lower in LRPs and followed a strict molecular clock, suggesting neutral genetic drift rather than positive selection. Additionally, polyfunctional CD8$^+$ T cell responses, particularly to TW10 and QW9 epitopes, were more robust in LRPs, who also showed significantly higher interleukin-2 (IL-2) production in early infection. Overall, the findings indicate that HLA-B*5701 patients with higher CD4 counts at baseline have a lower risk of HIV-1 disease progression because of the interplay between specific HLA-linked immune responses and the rate and mode of viral evolution. The study highlights the power of a multidisciplinary approach, integrating high-resolution evolutionary and immunological data, to understand mechanisms underlying HIV-1 pathogenesis.

In the absence of highly active antiretroviral therapy, most HIV-infected individuals progress to AIDS within 10 years. However, a proportion of patients (5 to 15%) can remain clinically and/or immunologically stable for years without therapy (11, 54, 61, 70). Among these are subjects who maintain high CD4$^+$ T cell counts for several years, with viremia usually ranging between 1,000 and 10,000 copies/ml (48), although many of them still show progressively increasing viral load (VL) and declining CD4$^+$ T cell counts (24, 35, 58, 65). It has been shown that the probability of progressing to AIDS for subjects with a baseline (i.e., within the first 6 months postinfection) VL around or less than 10,000 copies/ml is dependent on baseline CD4$^+$ T cell counts. Specifically, among patients with low plasma VL, those with baseline CD4$^+$ T cell counts of $<$750 cells/mm^3 are at significantly higher risk for progression to AIDS than those with CD4$^+$ T cell counts of $>$750 cells/mm^3 (45). There is also a small subset of subjects ($<$1%), known as elite controllers (ECs) or long-term nonprogressors (LTNPs), who have either undetectable VL or who maintain CD4$^+$ T cell counts of $>$500 cells/mm^3 for more than 10 years and HIV-1 RNA levels below the detection limit of conventional assays ($<$50 copies/ml) (48). A large proportion of LTNPs express the HLA class I allele B*5701 (48, 52). How this specific allele is associated with slow disease progression remains incompletely understood.

Interplay between viral replication and host immunity drives emergence of viral escape mutants (32) through accumulation of nonsynonymous mutations within immunodominant epitopes, a process that effectively determines the course of HIV-1 disease (4, 42). Escape mutations develop rapidly in HLA-B*5701-restricted epitopes in the acute phase of HIV-1 infection, even in individuals who achieve early control of viral replication (10). Several epitopes presented by HLA-B*5701 are located in the HIV-1 Gag polyprotein, which includes highly conserved components of the virion's capsid. The role of Gag in virion structure makes it difficult for escape mutations to develop without negatively affecting viral fitness, which likely increases the effectiveness of immune responses targeting this polyprotein (8, 38, 44, 76). There are four HLA-B*5701-restricted epitopes in Gag p24: ISW9 (termed Gag 147-155; HXB2 amino acid positions are used), KF11 (Gag 162-172), TW10 (Gag 240-249), and QW9 (Gag 308-316). Escape from ISW9-specific CD8$^+$ T cells is observed in the N-terminal flanking position (A146P/S), preventing cleavage to an optimal size for HLA binding (15), and within the epitope at position I147L (15, 63). The CD8$^+$ T cell response to the KF11 epitope is immunodominant during chronic infection (37). In the TW10 epitope, which is immunodominant in primary infection, there is a well-known early escape mutation (T242N), observed in almost all HLA-B*57 individuals (10), which disrupts critical interactions with the host protein cyclophilin A (CypA; Gag 213-230), resulting in a 10-fold reduction in viral replicative capacity (7). Two

Received 10 May 2012 **Accepted** 13 June 2012

Published ahead of print 3 July 2012

Address correspondence to Annika C. Karlsson, annika.karlsson@ki.se, or Marco Salemi, salemi@pathology.ufl.edu.

Supplemental material for this article may be found at http://jvi.asm.org/.

doi:10.1128/JVI.01165-12

TABLE 1 Patient characteristics

Patient	Class I HLA alleles	Baseline value			CD4 slope (% change/year)	Study period[b] (wpi)	Classification[c]
		Time point[a] (wpi)	VL (copies/ml)	CD4 (cells/mm^3)			
P1	A*0101, *0301; B*2705, *5701	10	7,728	555	−15.7	13–271	HRP
P2	A*0101, *2402; B*4002, *5701	10	4,973	570	−14.8	18–195	HRP
P3	A*2402, *3201; B*4002, *5701	10	<50	250	−3.6[e]	13–324	HRP
P4	A*0101, *0201; B*5101, *5701	10/11[d]	293	1,452	−7.0	11–316	LRP
P5	A*0101, *0101; B*0801, *5701	10	1,533	1,102	−6.4	13–309	LRP
P6	A*0301, *2402; B*3501, *5701	10	10,861	833	−5.9	10–377	LRP

[a] Date of the first available CD4 and VL measurements. The date of infection was estimated as the midpoint between reported seronegative and seropositive tests (see Materials and Methods for details).
[b] Time interval of longitudinal plasma and PBMC sampling for evolutionary and immunological analysis.
[c] Based on the CD4$^+$ T cell count at baseline with a threshold at 750 cells/mm^3. HRP, high-risk progressor (<750 cells/mm^3); LRP, low-risk progressor (>750 cells/mm^3) (45).
[d] Week 10 for VL and week 11 for CD4$^+$ T cell count measurement.
[e] Although P3 showed the slowest CD4 slope, the subject was still classified as HRP, since the subject also exhibited the lowest baseline CD4$^+$ T cell count, which remained, on average, at 400 cells/mm^3 during the study period.

mutations within the QW9 epitope (S310T and E312D) have been described, although it is unclear whether they represent actual escape mutations (49, 55).

The cytotoxic T lymphocyte (CTL) response has been associated with control of HIV-1 in HLA-B*5701 individuals. It has been shown that polyfunctional HIV-1-specific CD8$^+$ T cells in LTNPs/ECs maintain a high proliferative capacity that is coupled to increased interleukin-2 (IL-2) production (5, 12, 80) and preserved in HIV subjects with nonprogressive infections (50). Furthermore, IL-2 secretion by CD8$^+$ T cells has been linked to enhanced viral suppression in chronic HIV-1 controllers (1). Importantly, neither T cell receptor diversity nor clonality of the CD8$^+$ T cell response differs among HLA-B*5701 individuals who progress versus those who show markedly slower progression or long-term nonprogression (46).

A few studies have investigated viral diversity in HLA-B*5701 individuals in the context of epitope-specific CD8$^+$ T cell responses (3, 38, 49, 59, 75). Most studies have focused on correlates of protection by analyzing immunological profiles of LTNPs/ECs, where viral evolution is difficult to detect. The present work examined, for the first time, six HLA-B*5701 subjects who had not been treated, who had diverse rates of progression, and who were monitored longitudinally from early infection up to 7 years with detectable VL during the course of infection but had different CD4$^+$ T cell counts at baseline. Detailed Gag p24 evolutionary patterns, as well as specificity and quality of the epitope-specific CD8$^+$ T cell responses, were characterized with a multidisciplinary approach employing high-resolution phylogenetic analysis and polychromatic flow cytometry. Subjects with higher baseline CD4$^+$ T cell counts were characterized by more robust polyfunctional CD8$^+$ T cell responses toward specific HLA-B*5701-restricted epitopes and lower rates of viral evolution. Therefore, the data indicate that a lower risk of AIDS progression in HLA-B*5701 subjects might be explained, at least in part, by host immune responses constraining HIV-1 evolutionary pathways.

MATERIALS AND METHODS

Subjects and specimens. Six HLA-B*5701 participants were selected from the San Francisco-based HIV-1-infected cohort OPTIONS at the University of California (29) and were monitored from early infection up to 7 years (Table 1). Five of them were men who have sex with men (MSM), and one (P5) was an injecting drug user (IDU). Subjects P2 to P6 were treatment naïve, while P1 received antiretroviral treatment (ART) for 14 months (samples from the treatment period were excluded). Studies were performed on longitudinal plasma (stored at −80°C) and cryopreserved peripheral blood mononuclear cell (PBMC) samples (for details on the sampling scheme, see Fig. S1 in the supplemental material). For each subject, PBMC samples were studied from three time points. The sampling times were then classified within three different intervals, corresponding to the infection stage in estimated weeks postinfection (wpi): I_1 (<1 year; range, 13 to 39 wpi), I_2 (1 to 3 years; range, 109 to 157 wpi), and I_3 (>3 years; range, 195 to 377 wpi). In addition, CD4$^+$ T cell counts (cells/mm^3) and viral load (copies/ml) measurements were performed regularly during the course of infection. For each subject, the time since infection was estimated as the midpoint between reported negative and positive tests based on data from serologic tests (enzyme immunoassay [EIA], Western blotting, and less-sensitive EIA testing), HIV-1 RNA testing, and prior antibody testing history (20, 29, 30). Less-sensitive EIA testing was carried out using a version based on the Vironostika HIV-1 EIA (Organon Teknika Corporation). Estimated dates for antibody-negative or indeterminate subjects were based on the incubation period. The University of California, San Francisco (UCSF), Committee on Human Research and the Regional Ethical Council in Stockholm, Sweden (2008/1099-31), approved this study, and all patients provided written informed consent.

RNA extraction, cDNA synthesis, and PCR amplification. RNA extraction, viral cDNA synthesis, and PCR amplification were performed according to a slightly modified version of a previously described protocol (39). HIV-1 *gag* p24 sequences were amplified from viral cDNA by limiting-dilution digital nested PCR (single-genome sequencing) to prevent PCR resampling (33, 60). Sequences were assembled with Sequencher software and edited manually.

Data set assembling and evolutionary analysis. Subject-specific alignments, available from the authors upon request, were obtained with BioEdit software (http://www.mbio.ncsu.edu/bioedit/bioedit.html), and the HIV-1 subtype was assessed for each subject (13). A neighbor-joining phylogenetic tree was inferred for all sequences using MEGA5.0 (74) to exclude the possibility of contamination (see Fig. S2 in the supplemental material). Phylogenetic and recombination signals in each data set were investigated by likelihood mapping (71) and the PHI test-based algorithm (9, 68), using TREE-PUZZLE (69) and SplitsTree (31), respectively. The best-fitting nucleotide substitution model was selected with a hierarchical likelihood ratio test (73). Maximum likelihood (ML) trees were inferred with PhyML (28) and HIV-1 intrahost evolutionary rates were calculated with BEAST (17), under either a strict or relaxed molecular clock model (16), using the best-fitting demographic model for each data set (data not

shown). Positive selection was investigated by estimating the average number of synonymous and nonsynonymous substitutions, which were estimated with the Nei and Gojobori method (56), and by comparing different ML codon substitution models (57, 72, 77, 78) implemented in the codeml program of the PAML package (79). Full details on the evolutionary analysis are given in the supplemental material.

Immunological analysis. To study $CD8^+$ T cell responses, a panel of autologous HLA-B*5701-restricted epitopes located in Gag p24 was identified based on the individual sequences for each patient. PBMC stimulation and intracellular cytokine staining was performed. Cells were stained for Vivid, CD8, CD3, CD4, gamma interferon (IFN-γ), interleukin-2 (IL-2), macrophage inflammatory protein 1β (MIP-1β), and perforin. Flow cytometry analyses were performed on a standardized 8-color CantoII (BD Biosciences). A typical T cell gating was used to distinguish the $CD8^+$ T cell responses (see Fig. S4 in the supplemental material). Peptide-specific $CD8^+$ T cell responses were considered positive if the frequency of responding cells was more than twice the average negative background, and when background was high for a specific cytokine, different cytokines were plotted on *x* and *y* axes (64). The Boolean gating principle was applied to create combinational events of IFN-γ, IL-2, MIP-1β, and perforin to evaluate the functional diversities of epitope-specific $CD8^+$ T cell responses through SPICE (66). Statistical analyses were performed using Graphpad Prism 5.0 software as well as SAS v9.2 and Stata10. Full details are given in the supplemental material.

Nucleotide sequence accession numbers. The sequences determined in the course of this work have been deposited in GenBank under accession numbers JX234575 to JX235332.

RESULTS

Patient characteristics. Six HLA-B*5701 HIV-1 subtype B-positive men from the OPTIONS cohort (29) at University of California, San Francisco, were selected for this study (Table 1). All subjects were monitored from early infection (median time, 3 wpi; range, 10 to 18 wpi) up to 7 years (see Fig. S1 in supplemental material) and for a similar number of weeks (median, 300.5 weeks; range, 177 to 367; Table 1) while they remained untreated. At study enrollment, all subjects were at a similar stage of infection: five out of six subjects were Fiebig stage V (antibody test positive but p31 band negative by Western blotting), which typically indicates being within 75 days or less of antibody seroconversion on conventional HIV-1 antibody tests (20); the sixth subject (P4) had a positive p31 band (with a less-sensitive EIA standardized optical density of 0.20) which is consistent with being within 90 days of seroconversion (30).

As expected, all study subjects exhibited lower viral loads (VL) than are usually observed in non-HLA-B57 chronic or rapid progressors (40, 48), with VL of ≤10,000 copies/ml at baseline and fluctuations mostly between 1,000 and 10,000 copies/ml throughout the study period. Since all patients initiated treatment before the AIDS phase ($CD4^+$ T cell counts of <200 cells/mm^3), classifications based on rate of progression to AIDS could not be applied. However, a large multicenter cohort study has shown that HIV-1-infected subjects with baseline VL of ≤10,000 copies/ml have differential risks of progression to AIDS depending on their baseline $CD4^+$ T cell count (45). Subjects with <750 $CD4^+$ T cells/mm^3 are two to five times more likely to develop AIDS in 6 to 9 years. Within the cohort enrolled for the present study, the $CD4^+$ T cell count at baseline was <750 cells/mm^3 for P1 to P3 but >750 cells/mm^3 for P4 to P6 (Table 1). Therefore, in what follows, these two groups of subjects are referred to as high-risk progressors (HRPs) and low-risk progressors (LRPs), respectively. The analyses will show that each group was indeed characterized by clearly distinct immunological and virological patterns (see below).

$CD4^+$ T cell counts at baseline (10 to 11 wpi) were significantly different between HRPs and LRPs ($P = 0.032$ by *t* test; see Table S1 in supplemental material). LRPs consistently maintained higher $CD4^+$ T cell counts than HRPs throughout the duration of the study period, although the difference was no longer significant at the end, when all patients eventually progressed (see Fig. S1). In contrast, VL was not significantly different between the groups either at baseline or at the last sampled time point (see Table S1). The $CD4^+$ T cell slope for the HRPs generally was steeper than that for the LRPs (Table 1), with one exception (P3). This subject, however, displayed the lowest CD4 baseline value (250 cells/mm^3) while still fitting the criterion for classification within the HRP group.

Sequence variation in *gag* p24 HLA-B*5701-restricted epitopes and flanking regions over time. The highest frequencies of HIV-1-specific $CD8^+$ T cells in HLA-B*57^+ subjects are typically directed against the Gag protein (49). Therefore, plasma HIV-1 p24 single-genome sequences were obtained over time for HLA-B*5701 LRP and HRP subjects to investigate the interplay between genetic heterogeneity and antigen-specific immune control of virus replication.

Overall, nucleotide diversity in p24 was significantly higher in HRPs than in LRPs (Table 2). Six to 13 substitutions were observed between sequence pairs throughout the duration of the study in HRPs, but only 3 to 5 were observed in the LRPs ($P = 0.043$ by *t* test). Sequence variation in the four known HLA-B*5701-restricted epitopes, analyzed separately, showed two interesting patterns. First, for both groups of subjects the majority of pairwise substitutions were detected in the flanking regions rather than in the actual epitopes (Table 2). Second, in the flanking regions LRPs showed a significantly lower number of substitutions than HRPs ($P = 0.037$). The average number of pairwise synonymous and nonsynonymous substitutions was not significantly different within the HLA-B*5701-restricted epitopes in LRPs compared to HRPs (see Table S2 in supplemental material). Interestingly, however, the substitution frequency was significantly higher in the flanking regions for the HRPs than for the LRPs in the case of both synonymous ($P = 0.049$) and nonsynonymous substitutions ($P = 0.024$). The lower frequency of synonymous nucleotide changes in the HLA-B*5701 LRPs is in agreement with an earlier report describing the association between slow disease progression and the synonymous substitution rate of HIV-1, which may be linked to lower replication dynamics (36).

Specific mutations were mapped directly within p24 HLA-B*5701-restricted epitopes and flanking regions for both HRPs and LRPs (Fig. 1). Mutation in the QW9 epitope was detected in all HRPs (Fig. 1A). In subjects P1 and P3, the E312D mutation was present as the major viral population in ≥50% of the sampled time points. In HRP P2, the mutation S310T was detected in all single genomes at all sampled time points. On the other hand, no mutations were detected within the QW9 epitope (QASQEVKNW; Gag 308-316) in any of the LRPs, except from one single genome at one time point in P4 (Fig. 1B), in which case the mutation, K312D, corresponded to a minor viral variant (4.5%).

Interestingly, subject P1 also was HLA-B*2705^+, but the HLA-B*2705-restricted KK10 epitope was completely conserved in the viral sequences sampled at the first three time points (13 to 168

TABLE 2 Average number of pairwise substitutions and diversity in different groups of patients[c]

Patient group and no.	Avg. no. of substitutions and diversity in:					
	Gag p24 region		HLA-B*5701 epitope regions		Flanking regions	
	N^a	Diversity[b]	N^a	Diversity[b]	N^a	Diversity[b]
HRPs						
P1	8.58 (1.52)	0.013 (0.0023)	1.77 (0.75)	0.014 (0.006)	6.81 (1.48)	0.012 (0.002)
P2	6.27 (1.16)	0.0092 (0.0018)	1.19 (0.58)	0.01 (0.005)	5.08 (1.21)	0.009 (0.002)
P3	13.5 (2.00)	0.02 (0.0032)	1.92 (0.83)	0.016 (0.007)	11.56 (2.04)	0.021 (0.003)
LRPs						
P4	3.08 (0.81)	0.0045 (0.0013)	0.84 (0.48)	0.007 (0.004)	2.24 (0.74)	0.004 (0.001)
P5	4.15 (1.12)	0.006 (0.0016)	1.98 (1.69)	0.017 (0.008)	2.17 (0.62)	0.004 (0.001)
P6	4.77 (1.09)	0.007 (0.0015)	1.32 (0.68)	0.011 (0.006)	3.46 (0.86)	0.006 (0.001)
P value	**0.043**	**0.046**	0.335	0.357	**0.037**	**0.038**

[a] Average number of differences (including all time points). The standard errors, calculated by bootstrapping (500 replicates), are given in parentheses.
[b] Overall diversity (including all time points). The standard errors, calculated by bootstrapping (500 replicates), are given in parentheses.
[c] *P* values for LRPs versus HRPs were determined by *t* test, and significance ($P < 0.05$) is marked in boldface.

wpi), while one mutation was detected at the last time point (271 wpi) in only 3 (out of 22) of the sampled sequences. This finding is in agreement with the observation that selection pressure exerted on the virus to mutate the B*27-restricted KK10 epitope usually increases during the late stage of the infection (22).

Distinct mutation patterns between the two groups of patients were also observed within or upstream of the flanking regions of the epitope TW10 (TSTLQEQIGW; Gag 240-249). Two HRPs, P2 and P3, showed a different pattern consisting of subject-specific mutations T242N and T249X (X = A, E, or R) in TW10 (Fig. 1A). These two patients also had several mutations in the CypA-binding loop (DRVHPVHAGPIAPGQMRE; Gag 213-230), which increased in frequency over time. There are three known upstream compensatory mutations associated with the T242N mutation (H219Q, I223V, and M228I/L) that restore viral fitness and that are associated with an increase in plasma viral load (8). Upon closer inspection, there was a progressive increase in these compensatory mutations with increasing plasma viral loads for P3 but not for P2 (Fig. 1A). In two LRPs, P4 and P6, only the T242N mutation was detected as the major viral population over time (Fig. 1B).

Mutation patterns within flanking regions of the epitope ISW9 (ISPRITNAW; Gag 147-155) were similar in both LRPs and HRPs. All patients except for P2 had at least one mutation in ISW9. Responses targeting the HLA-B*5701-restricted epitope KF11 (KAFLRPEVIPMF; Gag 167-172) have been previously shown to be quantitatively immunodominant in HLA-B*5701 HIV-infected patients (25, 26, 47, 52). Interestingly, this sequence was completely conserved to the consensus clade B sequence in four patients, P2 to P5. Two patients, P1 and P6, developed mutations in KF11 during the chronic phase, and at the latest time point the major viral population contained the V168I mutation (Fig. 1).

Likelihood mapping analysis. Phylogenetic signal and phylogenetic noise in each Gag p24 alignment were quantified by likelihood mapping analysis (Fig. 2; also see Fig. S3 in supplemental material). In general, data sets showed <40% of the dots in the center of the likelihood maps, indicating a robust signal for phylogeny inference (71). However, an interesting pattern emerged. HLA-B*5701 subjects classified as HRPs showed consistently less intense star-like signals (13.8 to 16.1%) than LRPs (25.5 to 37.8%). This may be explained by a higher degree of homoplasy in such patients or more constrained mutational pathways, in agreement with the finding that HIV-1 intrahost evolution in LRP subjects was characterized by lower genetic heterogeneity (Table 2).

Phylogenetic analysis of longitudinally sampled *gag* p24 sequences. Phylogenetic analyses were carried out to investigate in greater detail HIV-1 evolutionary patterns. Recombination is known to occur at a high rate in HIV-1, and evolutionary inferences based on trees that include recombinant sequences can be severely misleading (68). Therefore, the identification and removal of eight sequences from subject P4 and two sequences from subject P1 was the initial step in the analysis. Sequences from the last three time points of subject P3 were also excluded, since they originated from several successful recombination events that established a new viral population with increased viral fitness (data not shown), and they were analyzed separately (unpublished data).

Several interesting patterns were evident in the maximum likelihood (ML) trees inferred from the six data sets (Fig. 3). Overall, the trees showed a staircase-like topology, which is consistent with the emergence of specific viral subpopulations over time through sequential population bottlenecks (27, 67). A certain degree of intermixing of sequences from different time points was evident, possibly due to archival viruses from infection of cellular reservoirs (6). For each tree, specific amino acid changes were mapped along statistically supported bottlenecks (bootstrap value of >65% and/or approximate likelihood ratio test, aLRT, $P > 0.75$). A closer look at the temporal succession of mutational events along the major bottlenecks of the viral quasispecies infecting LRPs revealed that the changes in TW10 and ISW9 (including upstream position 146) and the CypA-binding loop occurred in a specific order (Fig. 3, right). In all but one subject (P6), the virus displayed early bottleneck mutations in TW10, but in this subject the T242N escape variant was already present in all sequences since the first sampled time point (Fig. 3F). On the other hand, viral evolutionary patterns along population bottlenecks appeared to be less constrained in the HRP group and were characterized by the more frequent emergence of variants with amino acid replacements in the CypA-binding loop and/or other flanking regions

A HRPs

Patient ID	Weeks since infection	Single genomes	Proportion (%)	ISW9 (Gag 147-155)	KF11 (Gag 162-172)	CypA-binding loop (Gag 213-230)	TW10 (Gag 240-249)	QW9 (Gag 308-316)
Gag (HXB2)				AISPRTLNAWV	EKAFSPEVIPMFS	DRVHPVHAGPIAPGQMRE	TTSTLQEQIGWM	EQASQEVKNWM
P1	13	18/23	78	SL.....	.....	..L.....	.....	.....D.....
		2/23	9	SL.....	.....	..L.....	.....R.....	.....D.....
		2/23	9	SL.....	.....	..L.....	.....E..	.....D.....
		1/23	4	SL.....	.....	..L.....	...N.....	.....D.....
	104	14/18	78	SL.....	.....	..L.....	...N.....	.....D.....
		3/18	17	PL.....	.....	..L.....	...N.....	.....D.....
		1/18	5	SL.....	.....S.	..L.....	...N.....	.....D.....
	168	15/29	52	PL.....	.....	..L.....	...N.....	.....D.....
		9/29	31	SL.....	.....	..L.....	...N.....	.....D.....
		2/29	7	PL.....	.....	..L.....	...N.....	.....
		1/29	3	PL.....	.....T.	..L.....	...N.....	.....
		1/29	3	PL.....	.....	..L...Q.....	...N.....	.....D.....
		1/29	3	PL.....	.....	..L...Q.....	...N.....	.....
	271	12/22	55	SL.....	.....I.....	..L...Q.....	...N.....	.....
		3/22	13.5	PL.....	.....T.	..L...Q.....	...N.....	.....
		3/22	13.5	SL.....	.....T.	..L.....	...N.....	.....
		2/22	9	.L.....	.....T.	..L...Q.....	...N.....	.....
		1/22	4.5	PL.....	.....T.	..L.....	...N.....	.....
		1/22	4.5	SL.....	.....I.....	..L.....	...N.....	.....
P2	18	27/28	96	.....	.....	.....Q.....	...N.....	.....T.....
		1/28	4	.....	.....	.....Q.....	...S.....	.....T.....
	109	21/23	91	.....	.....	..M...Q.....	...N.....	.....T.....
		1/23	4	.....	.....	..L..AQ.....	...N.....	.....T.....
		1/23	4	.....	.....	.....Q.....	...N.....	.....T.....
	195	17/28	61	.....	.....	..L..AQ.....I..	...N.....R..	.....T.....
		9/28	32	.....	.....	.....AQ.....I..	...N.....R..	.....T.....
		1/28	3.5	.....	.....	..L..AQ.....S..I..	...N.....R..	.....T.....
		1/28	3.5	.....	.....	..L..AQ.....I..	...N.....T..	.....T.....
P3	13	9/21	43	.....	.....	.....	.....A..	.....
		6/21	29	.....	.....	.....	.....E..	.....
		4/21	19	.....	.....	.....	...N.....	.....
		1/21	4.5	.....	.....	.....Q.....	.....A..	.....
		1/21	4.5	.....	.....	.....	.....	.....
	26	32/34	94	.....	.....	.....	.....A..	.....
		2/34	6	.....	.....	.....	...N.....	.....
	45	23/26	88	.....	.....	.....	...N.....	.....
		2/26	8	.....	.....	.....	...N.....A..	.....
		1/26	4	..L.....	.....	.....	...N.....	.....
	75	21/28	75	.....	.....	.....	...N.....A..	.....
		5/28	18	.L.....	.....	.....	...N.....A..	.....
		1/28	3.5	.....	.....	.....	.....A..	.....
		1/28	3.5	.....	.....	.....I..	...N.....A..	.....
	179	12/32	37.5	P.....	.....	.....	...N.....A..	.....D.....
		6/32	19	P.....	.....	..L.....	...N.....A..	.....D.....
		6/32	19	P.....	.....	..L.....V....I..	...N.....A..	.....
		5/32	15.5	P.....	.....	..L.....V....I..	...N.....A..	.....D.....
		2/32	6	P.....	.....	..M.....	...N.....A..	.....D.....
		1/32	3	PL.....	.....	..L.....V....I..	...N.....A..	.....
	274	11/25	44	P.....	.....	..L.....V....I..	...N.....A..	.....D.....
		8/25	32	P.....	.....	..L.....	...N.....A..	.....D.....
		3/25	12	P.A.....	.....	..L...Q.....	...N.....A..	.....D.....
		2/25	8	P.A.....	.....	..L.....L..	...N.....A..	.....D.....
		1/25	4	.....	.....	..L...Q.....I..	...N.....A..	.....D.....
	324	13/27	48	P.....	.....	..L.....V....I..	...N.....A..	.....D.....
		10/27	37	P.....	.....	..L.....	...N.....A..	.....D.....
		3/27	11	P.A.....	.....	..L.....L..	...N.....A..	.....D.....
		1/27	4	P.....	.....	..L.....L..	...N.....A..	.....D.....

FIG 1 Sequence variation in the four Gag p24 HLA-B*5701-restricted epitopes (ISW9, KF11, TW10, and QW9) and the CypA-binding loop for HRPs (A) and LRPs (B). HXB2 (top) is used as the reference sequence. Amino acid residues defining the epitopes and the compensatory mutations for TW10 in the CypA-binding loop are marked in boldface. The relative positions for each epitope and the CypA-binding loop are in parentheses.

B LRPs

Patient ID	Weeks since infection	Single genomes	Proportion (%)	ISW9 (Gag 147-155)	KF11 (Gag 162-172)	CypA-binding loop (Gag 213-230)	TW10 (Gag 240-249)	QW9 (Gag 308-316)
Gag (HxB2)				AISPRTLNAWV	EKAFSPEVIPMFS	DRVHPVHAGPIAPGQMRE	TTSTLQEQIGWM	EQASQEVKNWM
P4	11	28/33	85	.....	.....	.....Q.....	...N.....	.....
		5/33	15	.....	.....	.....Q.....	...N.....A..	.....
	60	15/22	68	.....	.....	.....Q.....	...N.....	.....
		2/22	9.5	P.T.....	.....	.....Q.....	...N.....	.....
		1/22	4.5	..T.....	.....	.....Q.....	...N.....	.....
		1/22	4.5	P.....	.....	.....Q.....	...N.....	.....
		1/22	4.5	.....	.....	..A...Q.....	...N.....	.....
		1/22	4.5	.....	.....	...Q..Q.....	...N.....	.....
		1/22	4.5	.....	.....	.....Q.....	...N.....	.....K.....
	157	19/19	100	P.....	.....	.....Q.....	...N.....	.....
	227	24/34	71	P.T.....	.....	.....Q.....	...N.....	.....
		9/34	26	P.....	.....	.....Q.....	...N.....	.....
		1/34	3	.....	.....	.....Q.....	...N.....	.....
	316	11/22	50	P.T.....	.....	.....Q.....	...N.....	.....
		6/22	27	.....	.....	.....Q.....	...N.....	.....
		5/22	23	PLT.....	.....	.....Q.....	...N.....	.....
P5	13	20/23	87	.....	.....	.....	.....	.....
		3/23	13	.....	.....	.....	.....E..	.....
	19	27/28	96	.....	.....	.....	.....E..	.....
		1/28	4	.....	.....	.....	.....	.....
	144	27/28	96	.....	.....	.....	...N.....A..	.....
		1/28	4	.....	.....	.....	.....A..	.....
	201	9/19	47	.L.....	.....	.....V.....	...N.....A..	.....
		7/19	37	.L.....	.....	.....	...N.....A..	.....
		2/19	11	.....	.....	.....	...N.....A..	.....
		1/19	5	.....	.....	.....V.....	...N.....A..	.....
	309	22/26	85	.L.....	.....	.....	...N.....A..	.....
		4/26	15	.L.....	.....	.....V.....	...N.....A..	.....
P6	10	26/27	96	.....	.....	..L.....	...N.....	.....
		1/27	4	P.....	.....	..L.....	...N.....	.....
	17	18/23	78	.....	.....	..L.....	...N.....	.....
		4/23	17	.L.....	.....	..L.....	...N.....	.....
		1/23	4	P.....	.....	..L.....	...N.....	.....
	183	23/23	100	.L.....	.....	..L...Q.....	...N.....	.....
	301	10/21	48	.L.....	.....	..L...Q.....	...N.....	.....
		10/21	48	.L.....	.....I.....	..L...Q.....	...N.....	.....
		1/21	4	.L.....	...S.....	..L...Q.....	...N.....	.....
	332	19/23	83	.L.....	.....I.....	..L...Q.....	...N.....	.....
		4/23	17	.L.....	.....	..L...Q.....	...N.....	.....
	377	14/23	61	.L.....	.....I.....	..L...Q.....	...N.....	.....
		7/23	30	.L.....	.....	..L...Q.....	...N.....	.....
		1/23	4	.L.....	.....T.	..L...Q.....	...N.....	.....
		1/23	4	.L.....	.....I.....	..L..AQ.....	...N.....	.....

FIG 1 continued

(Fig. 3, left). In one subject (P3), the T242N mutation along an early bottleneck reverted later on (Fig. 3C). The hypothesis that viral mutational pathways were restricted in HLA-B*5701 subjects classified as LRPs was strengthened by the higher degree of homoplasy (star-like signal) displayed in the likelihood maps of this group of patients (Fig. 2).

Selection and molecular clock analysis. The majority of the mutations occurring along the bottlenecks were within HLA-B*5701-restricted epitopes and the CypA-binding loop, suggesting that such mutations were associated with the successful emergence of the new subpopulation after each bottleneck. Significant positive selection at specific sites was tested using different site selection models for all six data sets (Table 3). Amino acid changes under significant selection, localized in internal branches of the ML trees along major bottlenecks (Fig. 3), were detected in two HRPs (P1 and P3). In P3, five sites were detected to be under positive selection, the majority of which were within TW10 and the CypA-binding loop (Fig. 3). In P1, two sites in flanking regions, one in the CypA-binding loop and one just outside the ISW9 epitope, were under positive selection. Neutral genetic drift models could not be rejected for P2 and the three LRP subjects. It is important to note that tests for selection tend to have limited power when applied to regions with low diversity, like p24. Therefore, it cannot be excluded that positive selection was, in fact, driving the evolution of fitter viral variants along most or all of the population bottlenecks observed in each tree. Interestingly, however, molecular clock analysis revealed that the 95% high-posterior-density (95% HPD) intervals of the coefficient of variation (CV) for data sets that did not display significant positive selection included zero. The CV is the evolutionary rate variance (estimated by a Bayesian relaxed molecular clock; see Materials and Methods) scaled by the associated mean. A 95% HPD en-

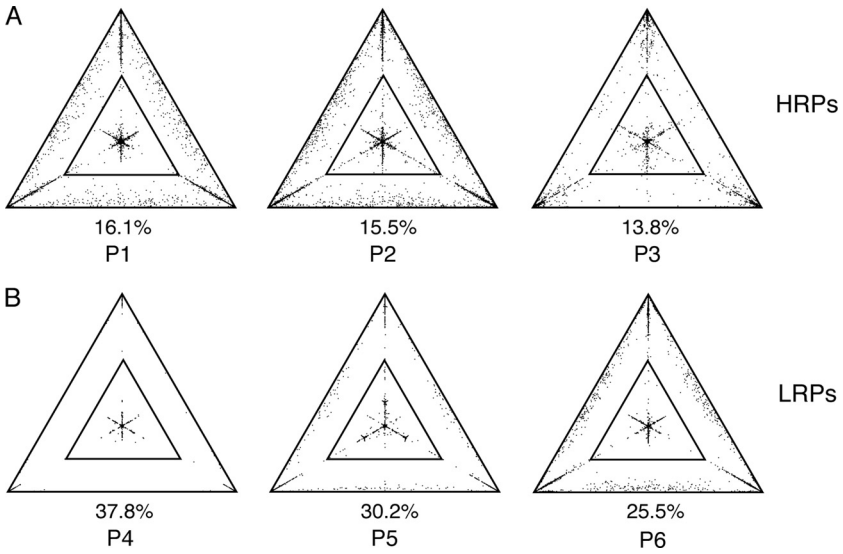

FIG 2 Likelihood mapping of HIV-1 Gag p24 sequences from different HLA-B*5701 subjects. Each dot represents the likelihoods of the three possible unrooted trees for a set of four sequences (quartets) selected randomly from the data set (see Materials and Methods). Dots close to the corners or the sides represent tree-like and network-like phylogenetic signals, respectively. The central area of the likelihood map, highlighted by a smaller triangle inside the map, represents a star-like signal. The higher the percentage of the dots (out of 10,000 random quartets) in the center of the triangle (given at the base of each map), the higher the phylogenetic noise in the data due to low genetic diversity and/or homoplasy. The spread of the data points in the remaining areas of the triangle carries little information, as long as these data points are equally distributed in each of the three corners (see Fig. S3 in the supplemental material). (A) Likelihood mapping of HIV-1 sequences sampled from HRP subjects. (B) Likelihood mapping of HIV-1 sequences sampled from LRP subjects.

compassing zero is evidence that the strict molecular clock cannot be rejected and suggests that evolution in HLA-B*5701 LRPs is driven by neutral genetic drift (34) rather than by positive selection, as in HRP subjects P1 and P3 (Table 3). However, failure to reject the strict clock does not necessarily imply that the relaxed-clock hypothesis is false, and the analysis cannot exclude the existence of different evolutionary rates in different parts of the tree driven by different level of selective pressures on different immunodominant epitopes.

HIV-1 intrahost evolutionary rates based on *gag* p24 longitudinally sampled sequences were compared among different subjects. A clear pattern emerged (Fig. 4) showing significantly faster median rates in HRPs than in LRPs ($P = 0.025$ by Mann-Whitney U-test). The result strengthened our confidence in the classification of these subjects within two distinct categories and indicated that viral evolution did occur at a lower rate in HLA-B*5701 subjects with a higher $CD4^+$ T cell count at baseline, in agreement with the constrained mutational patterns observed along the viral genealogies (see the previous section).

Polyfunctional HLA-B*5701-restricted $CD8^+$ T cell responses relate to risk of disease progression. The polyfunctional activity of $CD8^+$ T cells that produce multiple secreted effector molecules provides a strong correlate for efficacious control of viremia (2). Applying a Boolean gating scheme (see Fig. S4 in supplemental material), antigen-specific $CD8^+$ T cell responses were characterized longitudinally against the HIV-1-Gag p55 and p24 region using peptide pools. No statistically significant differences for Gag p55- and p24-specific $CD8^+$ T cells were distinguished between HRPs and LRPs (see Fig. S5 in supplemental material).

Functional diversity among $CD8^+$ T cell responses to the four HLA-B*5701-restricted wild-type epitopes was investigated between the LRPs and HRPs. LRPs displayed a broader functional profile than the HRPs, as demonstrated for responses to TW10 in subject P6 compared to those of subject P2 at I_1 (Fig. 5A). In general, data from other LRPs and HRPs were consistent among different time points. The LRPs showed a more robust $CD8^+$ T cell polyfunctionality toward the wild-type epitopes ($P < 0.001$) (Fig. 5B). In particular, $CD8^+$ T cells in the LRPs more frequently coexpressed IFN-γ and MIP-1β, as well as IFN-γ, MIP-1β, and IL-2 (Fig. 5C). In contrast, the $CD8^+$ T cell responses in the HRPs more frequently exhibited the ability to produce IFN-γ and perforin as well as IFN-γ, MIP-1β, and perforin (Fig. 5C). Finally, polyfunctionality was investigated at three different stages (<1, 1 to 3, and >3 years since infection) during the course of the disease. In both LRPs and HRPs, a decrease in $CD8^+$ T cell polyfunctionality toward the four HLA-B*5701-restricted wild-type epitopes was observed over time (Fig. 5D). A decrease in polyfunctionality was found in the HRP group between the first and last time interval ($P = 0.015$) due to a significant loss of cells producing IFN-γ, MIP-1β, and IL-2 ($P = 0.020$), as well as cells producing IFN-γ and IL-2 ($P = 0.033$) (data not shown). The same pattern was observed in the LRP group with a decrease in polyfunctionality between the first and second ($P = 0.023$) and the first and last time interval ($P = 0.042$). However, LRPs showed tendencies toward a higher polyfunctionality than the HRPs at the first time interval ($P = 0.062$) and significantly higher polyfunctionality at the second time interval ($P = 0.002$) (Fig. 5D). Overall, these results indicate that within the HLA-B*5701 study subjects, LRPs maintained higher $CD8^+$ T cell polyfunctionality during the first 3 years of infection compared to HRPs.

HLA-B*5701-restricted $CD8^+$ T cell responses to the TW10 and QW9 epitopes drive immunological differences related to risk of disease progression. The next step was to investigate whether the observed polyfunctional differences between LRPs and HRPs were predominantly driven by specific HLA-B*5701-

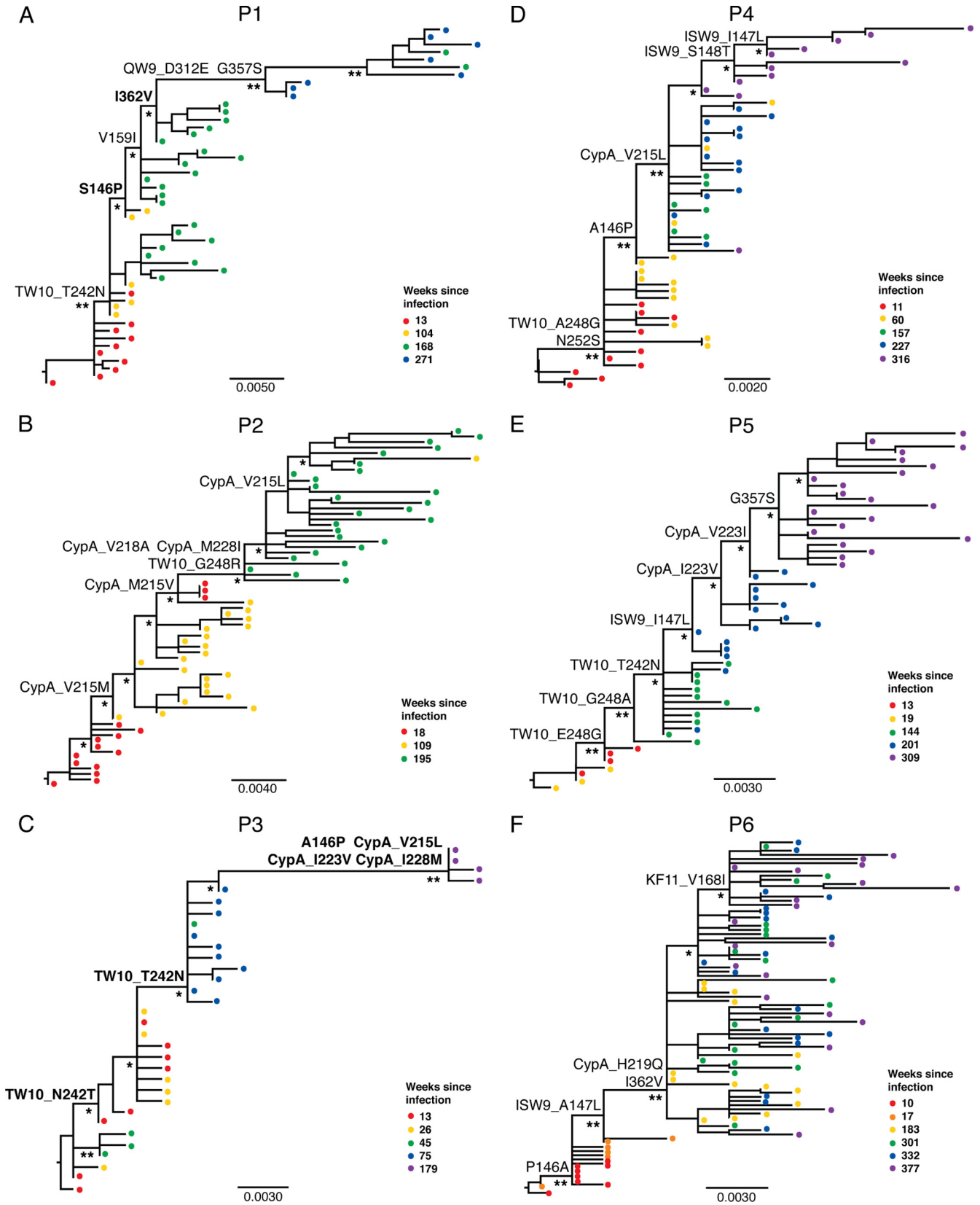

FIG 3 Maximum likelihood *gag* p24 genealogies (using only unique sequences) for HRPs (A to C) and LRPs (D to F). Strains sampled at different time points (estimated weeks from infection) are indicated by colored dots according to the legend in the figure. Branch lengths are drawn to scale in nucleotide substitutions per site according to the bar at the bottom of each tree. Statistical support for specific branches are indicated by one (bootstrap value of >65% or aLRT; $P > 0.75$) or two (bootstrap value of >65% and aLRT; $P > 0.75$) asterisks. Amino acid replacements along supported internal branches are indicated; the numbering refers to Gag amino acid positions in HXB2, which was used as the reference. Residues for which there is statistically significant evidence ($P > 95\%$) of positive selection are highlighted in boldface.

TABLE 3 Selection analysis and evolutionary rate variation in HIV-1 *gag* p24 longitudinal samples from all subjects

Patient group and no.	lnLK[a] (M8)	lnLK[b] (M8a)	M8a/M8[c] LR	Positively selected sites[d]	CV[e] (95% HPD)
HRPs					
P1	−1,427.3	−1,432.8	**11**	**146S, 362I**	1.06–3.91
P2	−1,578.3	−1,579.0	1.4		0–0.63
P3	−1,094.1	−1,095.7	**3.2**	**146A, 215V, 223I, 228 M, 242T**	3.57–5.05
LRPs					
P4	−1,258.0	−1,259.1	2.2		0–2.39
P5	−1,351.8	−1,353.0	2.4		0–1.47
P6	−1,717.6	−1,718.4	1.6		0–0.54

[a] Natural logarithm of the likelihood (lnLK) for the codon-based substitution M8 (positive selection; $dN/dS > 1$) model.
[b] lnLK for the codon-based substitution M8a (neutral; $dN/dS = 1$) model.
[c] Likelihood ratio (LR) statistic comparing M8a and M8. An LR of >2.71 indicates that the less complex (neutral) model, M8a, can be rejected (values in boldface). Similar results were obtained by comparing M8 to the less complex (neutral) model M7.
[d] According to the M8 model. Numbering refers to Gag amino acid positions in HXB2. Residues for which there is statistically significant evidence ($P > 95\%$) of positive selection are in boldface.
[e] Data are 95% high posterior density intervals (95% HPD) of the HIV-1 p24 evolutionary rate coefficient of variation (CV); 95% HPD intervals including zero (in boldface) indicate that the strict-clock hypothesis cannot be rejected.

restricted epitopes. No statistically significant differences were found between the two groups of patients for the wild-type ISW9 and KF11 epitopes, although tendencies toward higher polyfunctionality were observed in the LRPs (Fig. 6A). Interestingly, however, LRPs showed more robust polyfunctionality than HRPs against the wild-type QW9 ($P = 0.005$) and TW10 ($P = 0.033$) epitopes (Fig. 6A). Increased polyfunctionality was driven by a higher fraction of $CD8^+$ T cells producing IFN-γ, IL-2, and MIP-1β simultaneously (Fig. 6B), which was significantly higher in LRPs than HRPs for both QW9 ($P = 0.035$) and TW10 ($P = 0.024$) (Fig. 6C). Because LRPs and HRPs showed polyfunctionality toward the four HLA-B*5701-restricted wild-type epitopes during the course of infection, the $CD8^+$ T cell responses against the major autologous viral variants (Fig. 2) were investigated. The quality and magnitude of responses against autologous variants for all four epitopes showed a decline in polyfunctionality between the first and last time interval for both HRPs ($P = 0.005$) and LRPs ($P = 0.002$), which is in agreement with wild-type-specific responses. There was a significantly higher polyfunctionality in LRPs than HRPs at the first time interval ($P = 0.044$) (Fig. 6D). By examining functional combinations, LRPs again showed a higher degree of simultaneous IFN-γ, IL-2, and MIP-1β ($P = 0.013$) production compared to the HRPs (data not shown). This indicates that the $CD8^+$ T cell polyfunctionality toward autologous epitopes was higher in LRPs than HRPs during early infection.

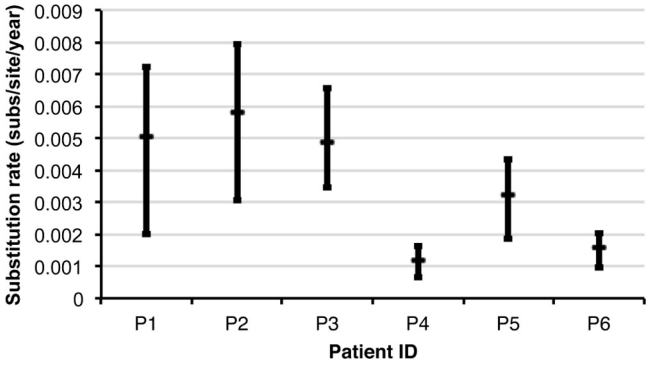

FIG 4 Median nucleotide substitution rate and 95% HPD intervals of HIV-1 Gag p24 in six longitudinally sampled HLA-B*5701 subjects. Substitution rates are given in nucleotide substitutions/site/year along the *x* axis and were estimated by Bayesian inference, assuming either a strict or relaxed molecular clock depending on the best-fitting model of each subject (Table 3). Substitution rates in the HRP group (P1 to P3) are significantly higher ($P = 0.025$ by Mann-Whitney U-test) than those in the LRP group (P4 to P6).

Distinct patterns of IL-2 production and correlation to $CD4^+$ T cell count in LRPs and HRPs. The fraction of $CD8^+$ T cells producing single markers toward the wild-type HLA-B*5701-restricted epitopes at each time interval was further investigated. In both HRPs and LRPs, the fraction of $CD8^+$ T cells producing IL-2 consistently declined over time and was significantly lower between the first and last time interval for both groups of patients (Fig. 7A). The fraction of $CD8^+$ T cells producing IL-2 was significantly higher in LRPs than in HRPs at the first ($P = 0.015$) and second ($P = 0.05$) time intervals. Interestingly, a significant correlation was found between IL-2-producing $CD8^+$ T cells in response to wild-type epitopes and $CD4^+$ T cell counts ($r = 0.28$; $P = 0.027$) but not VL (Fig. 7B). The finding suggests that initial $CD4^+$ T cell levels (i.e., >750 cells/mm^3) play an important role in preserving IL-2^+ $CD8^+$ T cell responses.

DISCUSSION

Defining correlates of protection is one of the greatest challenges in HIV-1 vaccine design. A mounting body of evidence has shown that HIV-1-specific $CD8^+$ T cell responses mediate immunologic control in HLA-B*5701 subjects with slower progression to AIDS (21, 26, 48, 52, 62). Most studies have focused on the magnitude and frequency of immune responses in LTNPs/ECs (14, 26, 44) or characterized the emergence of escape mutations within immunodominant epitopes in the Gag p24 region (3, 48), although ongoing viral intrahost evolution is difficult to characterize due to low viral copy numbers and genetic heterogeneity (54). However, it is the interplay between HIV-1 evolution and the host immune repertoire that determines the course of disease (42), and it may be insufficient to focus separately on immunological or evolutionary patterns for correlates of protection.

The present work focused on a unique cohort of six untreated HIV-1-infected subjects, all carrying the HLA-B*5701 allele,

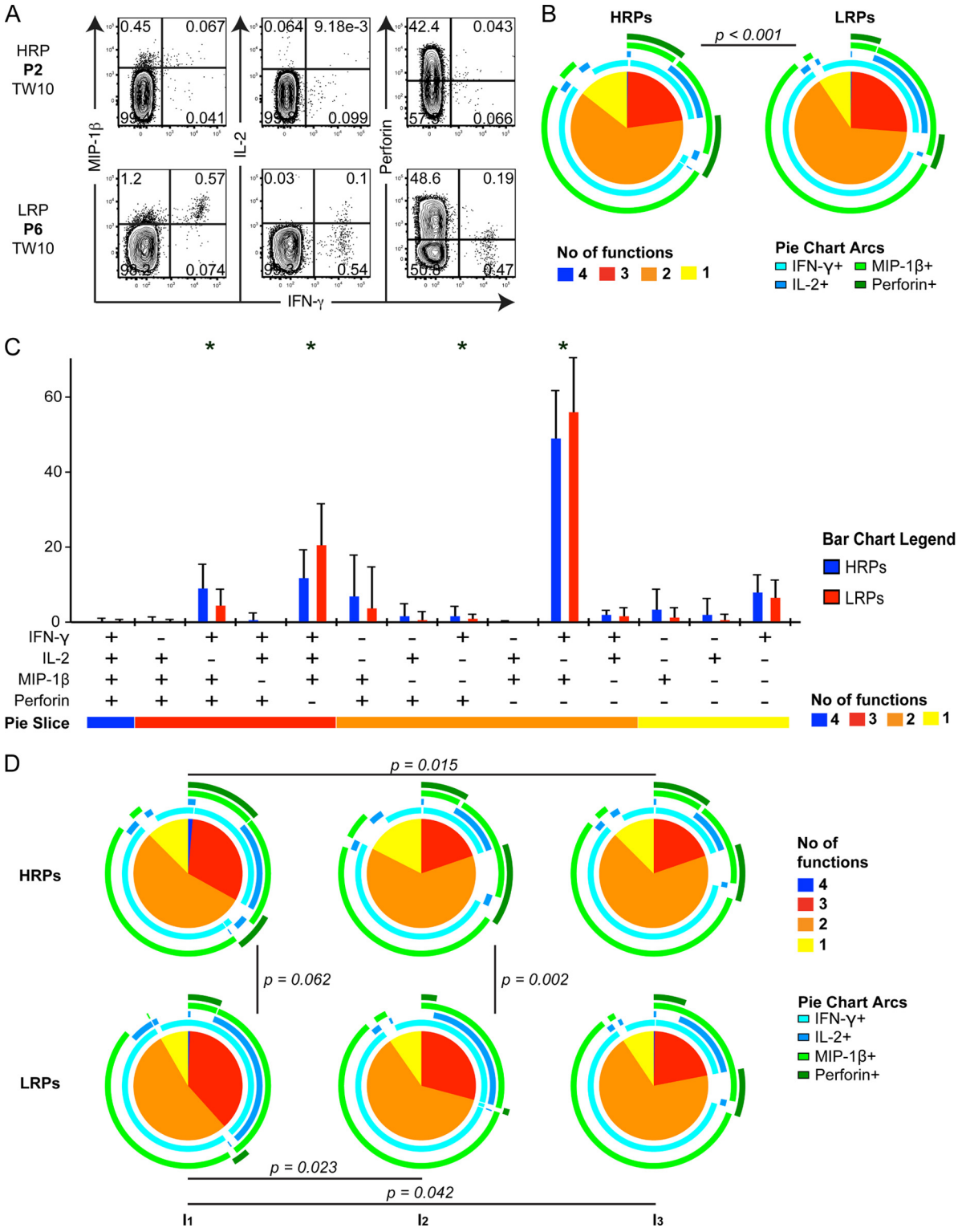

FIG 5 Functional discrepancies of CD8$^+$ T cell responses to wild-type HLA-B*5701-restricted epitopes in HRPs compared to LRPs. (A) Flow cytometry plots illustrating polyfunctional CD8$^+$ T cell responses to the TW10 epitope for representative HRP and LRP subjects. (B) Pie charts representing the proportion of CD8$^+$ T cell functions induced by the four wild-type HLA-B*5701-restricted epitopes (average response of the three time intervals for each subject). One to four functions are illustrated by the colors yellow, orange, red, and blue, respectively. The round bars surrounding the pie charts indicate diverse functions as indicated by the pie chart arcs. *P* values refer to permutation tests performed to compare the differences between the pie charts. (C) Frequency comparison of the functions of HLA-B*5701-restricted CD8$^+$ T cell responses in HRPs (blue) and LRPs (red) for each of the 14 potential combinations. The bars represent means and interquartile ranges (IQR). Significant differences between the bars for HRPs and LRPs are represented by an asterisk, which indicates $P < 0.05$ using Student's *t* test. (D) Pie charts demonstrating the functional diversity of longitudinal CD8$^+$ T cell responses to the four HLA-B*5701-restricted wild-type epitopes between HRPs and LRPs at each of the three time intervals (I_1 to I_3). The round bars surrounding the pie charts indicate various functions as indicated by the pie chart arcs. *P* values refer to permutation tests performed to compare the differences between the pie charts.

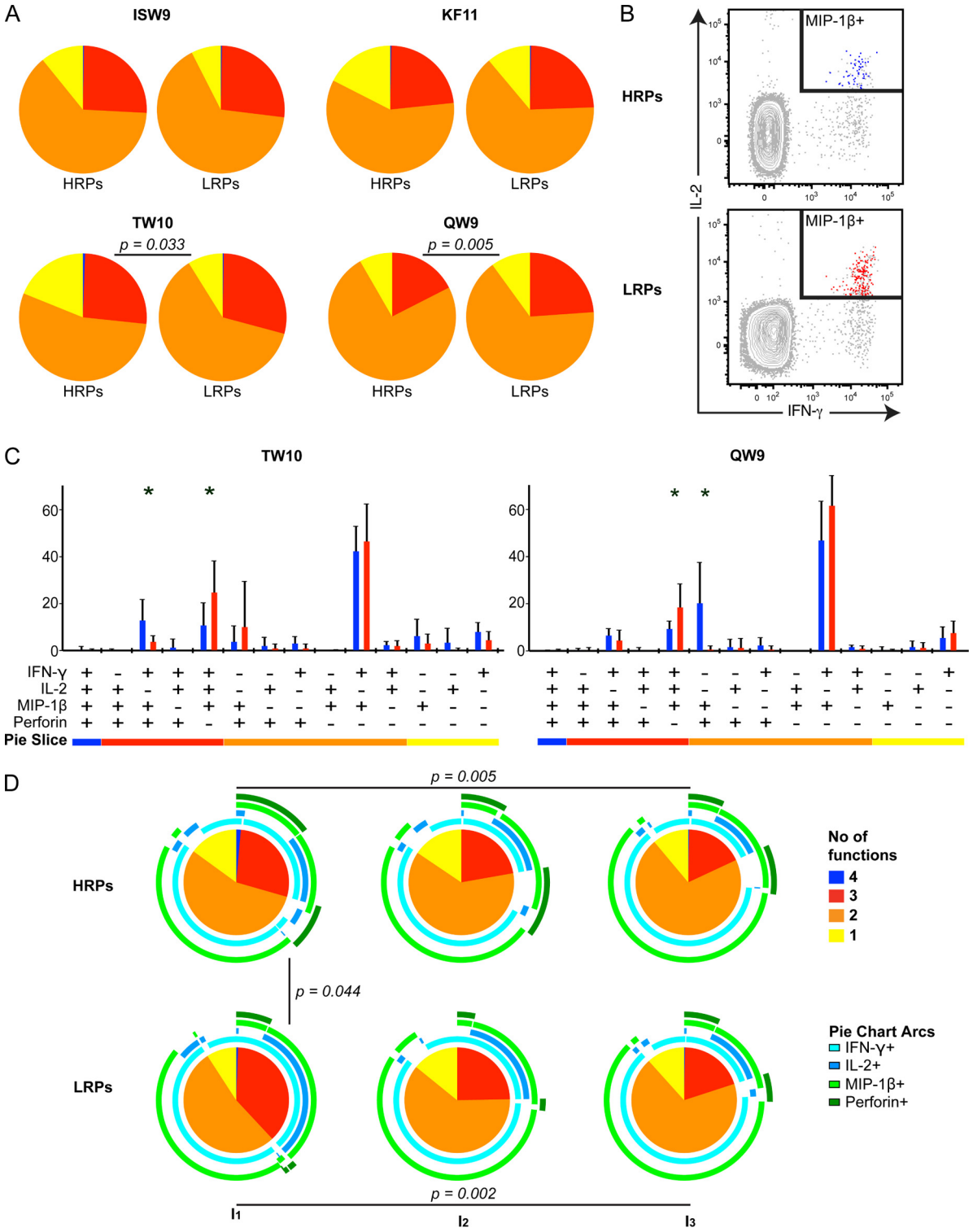

FIG 6 Functional discrepancies of QW9- and TW10-specific CD8$^+$ T cell responses between HRPs and LRPs. (A) Pie charts representing the fraction of CD8$^+$ T cell responses to each specific HLA-B*5701-restricted wild-type epitope. One to four functions are illustrated by the colors yellow, orange, red, and blue, respectively. Permutation tests were performed to compare the differences between the pie charts. (B) Representative flow cytometry plots demonstrating CD8$^+$ T cells producing IFN-γ, IL-2, and MIP-1β simultaneously (colored events represent those cells producing MIP-1β among gated IFN-γ/IL-2 double-positive cells). (C) Frequency comparison of the functional profile of QW9- and TW10-specific polyfunctional CD8$^+$ T cell responses in HRPs (blue) and LRPs (red) for each of the functional combinations. The bars represent the means and IQR. Significant differences between the bars are represented by an asterisk, which indicates $P < 0.05$ using Student's *t* test. (D) Pie charts demonstrating polyfunctional activity of CD8$^+$ T cell responses to the four HLA-B*5701-restricted major autologous variants between HRPs and LRPs at each of the three time intervals (I_1 to I_3). The round bars surrounding the pie charts indicate various functions as indicated by the pie chart arcs. *P* values refer to permutation tests performed to compare the differences between the pie charts.

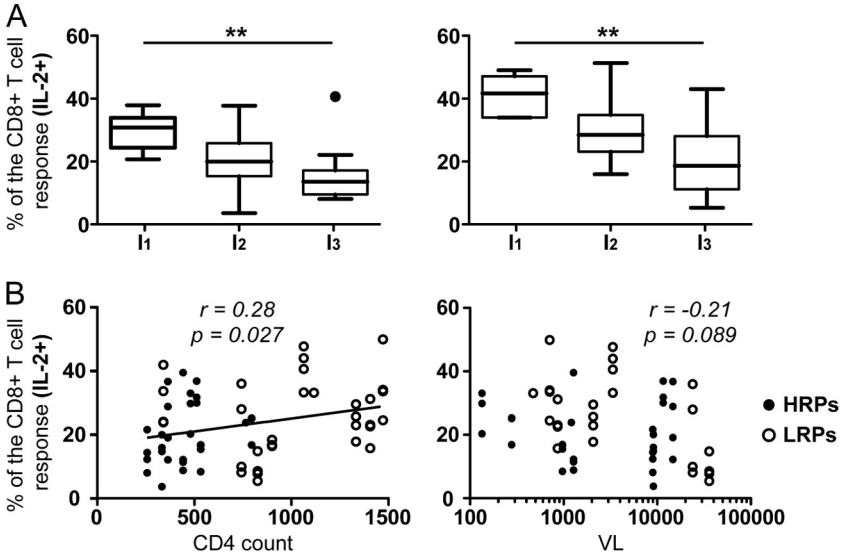

FIG 7 IL-2 production by CD8$^+$ T cells is associated with CD4$^+$ T cell counts. (A) Box-and-whisker plots (Tukey) demonstrating the longitudinal production of IL-2 for HRPs (left) or LRPs (right). *P* values (**, $P < 0.01$) were obtained from a one-way analysis of variance and a nonparametric Kruskal-Wallis test with Dunn's multiple comparison tests to compare all pairs of columns. (B) Correlation analysis between the average production of IL-2 and CD4 counts or VL for all subjects using the Spearman nonparametric test.

monitored longitudinally from early infection up to 7 years. All subjects had detectable VL during the study period and displayed sufficient phylogenetic signal for a robust evolutionary analysis. Study subjects were classified as HRPs or LRPs on the basis of their VL and CD4$^+$ T cell counts at baseline (10 to 11 wpi). Such a classification is supported by a robust multicenter cohort study of CD4$^+$ T cell counts and VL as prognostic markers of HIV-1 infection (45). Indeed, the comparison of HIV-1 Gag p24 evolutionary dynamics, as well as multifunctional CD8$^+$ T cell responses, between HRP and LRP subjects clearly showed distinct virological and immunological patterns.

HLA-B*5701 subjects with a baseline of >750 CD4$^+$ T cells/mm^3 (LRPs) were characterized by the gradual emergence of variants during sequential population bottlenecks (18, 53, 75) along restricted pathways. No mutants were detected in the QW9 epitope, possibly due to strong purifying selection, while mutations in ISW9, TW10, and CypA appeared to be driven by genetic drift rather than positive selection. Most importantly, HIV-1 p24 evolution appeared to follow a strict molecular clock, further evidence of neutrality, with a significantly lower evolutionary rate in LRPs than HRPs. Subjects with low baseline CD4$^+$ T cell counts (HRPs) displayed viral quasispecies evolving along less constrained mutational patterns, characterized by a relaxed molecular clock, higher median evolutionary rates, more changes in flanking regions, and the eventual emergence of QW9 variants, driven (at least in two patients) by positive selection. Viral escape and compensatory mutations in the TW10-restricted epitope and the CypA-binding loop region were detected in all six patients. These mutations disrupt critical interactions with the host protein CypA that result in a reduction in viral replicative capacity (7) and may be partially restored by compensatory substitutions in flanking regions (8). In agreement with the general findings of this study, the highest number of compensatory mutations was again observed in the two progressing patients that had the lowest CD4$^+$ T cell counts later in infection.

The evolutionary findings could be explained by the parallel observation that polyfunctional CD8$^+$ T cell responses toward wild-type HLA-B*5701-restricted epitopes, especially during the first and second time interval (up to 157 wpi), were significantly higher in LRPs. Polyfunctional CD8$^+$ T cell responses coproducing IFN-γ, MIP-1β, and IL-2 toward QW9 and TW10, as well as the fraction of IL-2-producing CD8$^+$ T cells, in response to wild-type epitopes were significantly higher in LRPs. Finally, CD8$^+$ T cell responses coproducing IFN-γ, MIP-1β, and IL-2 toward autologous epitopes were also significantly higher in LRPs at the first time interval early in infection. In other words, our results indicate that HIV-1 evolution in HLA-B*5701 patients with a high baseline CD4$^+$ T cell count was constrained by polyfunctional CD8$^+$ T cell responses with a maintained ability to coproduce IL-2. This notion is strengthened by a significant positive correlation between the fraction of IL-2-producing CD8$^+$ T cells and CD4$^+$ T cell count, which in turn could be associated with a lower viral evolutionary rate and risk of disease progression. Several studies have underlined the important role of IL-2-producing CD8$^+$ T cell functional subsets to mediate protective immunity at different stages of infection (12, 41, 43). In a recent review, Makedonas and Betts (42) suggest that IL-2 production enhancement of a central memory-type profile is necessary to maintain a healthy antiviral CD8$^+$ T cell population. Interestingly, IL-2 production by polyfunctional CD8$^+$ T cells has been linked to proliferative capacity (5, 12, 80), ability to upregulate perforin (50, 51), and enhanced viral suppression in chronic HIV-1 controllers (1). Taking these findings together, it is likely that differing capacities of CD8$^+$ T cells in LRPs versus HRPs to produce IL-2 would also influence their cytotoxic activity after proliferation and, in turn, the immune pressure on the virus. However, this has not directly been evaluated in our study, and it has also been proposed that mechanisms other than cytotoxicity could be exerting immune pressure during acute infection (19).

Overall, the findings suggest that polyfunctional CD8$^+$ T cell

responses with specific functional profiles are the cause of different viral evolutionary rates in HLA-B*5701 subjects with different baseline $CD4^+$ T cell counts. However, we do recognize that constrained HIV-1 evolution could be the result of other immunologic events which subsequently affect $CD8^+$ T cell polyfunctionality. In particular, the role of individual responses restricted by alleles other than HLA-B*5701 cannot be excluded. It should also be noted that even though we included more HLA-B*5701 patients than in previous studies, our sample size remains small. Therefore, the lack of significance for some of the comparisons might be due to a lack of statistical power.

While no single function of HIV-1-specific $CD8^+$ T cells explains control of HIV-1 replication, evolution, or overall disease progression (42), $CD8^+$ T cell polyfunctionality provides a measurable correlate of control in HIV-1 infection (2, 5). The course of HIV-1 disease most likely is determined by interaction between viral replication immediately after infection and the host immune response (23), both innate and adaptive (42). It has also been shown that disease progression is better defined by the presence of HLA-B*57-restricted HIV-specific $CD8^+$ T cell responses after primary infection (14). Unfortunately, samples for these patients were only available at 10 to 18 wpi, following the earliest events of acute infection. Nonetheless, significant differences in the HLA-B*5701-specific $CD8^+$ T cell responses between LRPs and HRPs were clearly observed relatively early in infection (during the first time interval, 13 to 39 wpi). This difference suggests a link between the ability of the immune system to constrain HIV-1 evolution along restricted mutational pathways and a longer persistence of high $CD4^+$ T cell counts in the LRPs. Previous studies have failed to find a correlation between the development of specific escape mutations and disease progression (18). This is, perhaps, not surprising if we consider the combinatorial explosion of possible mutations within HLA-restricted epitopes, which may contribute to immune escape, and in flanking regions, which may compensate for reduced viral fitness. Moreover, it cannot be excluded that additional mutations outside the Gag region also contribute to the successful propagation/survival of the viral quasispecies.

In conclusion, the present study provided insights into the roles of polyfunctional $CD8^+$ T cells and IL-2-producing T cells in constraining the tempo and mode of HIV-1 evolution in HLA-B*5701 subjects. This suggests that these biomarkers provide additional measures of risk for disease progression, including both viral evolutionary dynamics and host immune responses, that are essential for the development of an effective vaccine (42). The study also demonstrates the power of a multidisciplinary approach that combines evolutionary and immunological data to understand host-pathogen interactions and dynamics of HIV-1 pathogenesis, which could be expanded to other fast-evolving viruses.

ACKNOWLEDGMENTS

This work was supported by grants from the Swedish Research Council (K2010-56X-20345-04-3), Swedish Agency for International Development Cooperation-SIDA (2005-001756), Erik and Edith Fernströms foundation, Karolinska Institutet, Åke Wibergs Foundation (40418186), and the Swedish Society of Medicine (SLS-101021). M.M.N., M.B., and J.T. are supported by partial funding of new postgraduate students at Karolinska Institutet. M.S. is supported in part by NIH grant R01 NS063897-01A2. The employment of A.C.K. as a senior researcher is supported by grants from the Karolinska Institutet.

We are particularly thankful to Douglas F. Nixon for critical reading of the manuscript, to Bruno Vanherberghen for proofreading the manuscript, to Sarah E. Palmer for providing expertise on single genome sequencing, and to the study subjects for providing samples.

REFERENCES

1. **Akinsiku OT, Bansal A, Sabbaj S, Heath SL, Goepfert PA.** 2011. Interleukin-2 production by polyfunctional HIV-1-specific CD8 T cells is associated with enhanced viral suppression. J. Acquir. Immune Defic. Syndr. **58**:132–140.
2. **Almeida JR, et al.** 2007. Superior control of HIV-1 replication by CD8+ T cells is reflected by their avidity, polyfunctionality, and clonal turnover. J. Exp. Med. **204**:2473–2485.
3. **Bailey JR, Williams TM, Siliciano RF, Blankson JN.** 2006. Maintenance of viral suppression in HIV-1-infected HLA-B*57+ elite suppressors despite CTL escape mutations. J. Exp. Med. **203**:1357–1369.
4. **Bailey JR, et al.** 2007. Evolution of HIV-1 in an HLA-B*57-positive patient during virologic escape. J. Infect. Dis. **196**:50–55.
5. **Betts MR, et al.** 2006. HIV nonprogressors preferentially maintain highly functional HIV-specific CD8+ T cells. Blood **107**:4781–4789.
6. **Blankson J, Persaud D, Siliciano RF.** 1999. Latent reservoirs for HIV-1. Curr. Opin. Infect. Dis. **12**:5–11.
7. **Borghans JA, Molgaard A, de Boer RJ, Kesmir C.** 2007. HLA alleles associated with slow progression to AIDS truly prefer to present HIV-1 p24. PLoS One **2**:e920. doi:10.1371/journal.pone.0000920.
8. **Brockman MA, et al.** 2007. Escape and compensation from early HLA-B57-mediated cytotoxic T-lymphocyte pressure on human immunodeficiency virus type 1 Gag alter capsid interactions with cyclophilin A. J. Virol. **81**:12608–12618.
9. **Bruen TC, Philippe H, Bryant D.** 2006. A simple and robust statistical test for detecting the presence of recombination. Genetics **172**:2665–2681.
10. **Brumme ZL, et al.** 2008. Marked epitope- and allele-specific differences in rates of mutation in human immunodeficiency type 1 (HIV-1) Gag, Pol, and Nef cytotoxic T-lymphocyte epitopes in acute/early HIV-1 infection. J. Virol. **82**:9216–9227.
11. **Cao Y, Qin L, Zhang L, Safrit J, Ho DD.** 1995. Virologic and immunologic characterization of long-term survivors of human immunodeficiency virus type 1 infection. N. Engl. J. Med. **332**:201–208.
12. **Cellerai C, et al.** 2010. Proliferation capacity and cytotoxic activity are mediated by functionally and phenotypically distinct virus-specific CD8 T cells defined by interleukin-7Rα (CD127) and perforin expression. J. Virol. **84**:3868–3878.
13. **de Oliveira T, et al.** 2005. An automated genotyping system for analysis of HIV-1 and other microbial sequences. Bioinformatics **21**:3797–3800.
14. **Dinges WL, et al.** 2010. Virus-specific CD8+ T-cell responses better define HIV disease progression than HLA genotype. J. Virol. **84**:4461–4468.
15. **Draenert R, et al.** 2004. Immune selection for altered antigen processing leads to cytotoxic T lymphocyte escape in chronic HIV-1 infection. J. Exp. Med. **199**:905–915.
16. **Drummond AJ, Ho SY, Phillips MJ, Rambaut A.** 2006. Relaxed phylogenetics and dating with confidence. PLoS Biol. **4**:e88. doi:10.1371/journal.pbio.0040088.
17. **Drummond AJ, Suchard MA, Xie D, Rambaut A.** 2012. Bayesian phylogenetics with BEAUti and the BEAST 1.7. Mol. Biol. Evol. [Epub ahead of print.] doi:10.1093/molbev/mss075.
18. **Durand CM, et al.** 2010. HIV-1 Gag evolution in recently infected human leukocyte antigen-B*57 patients with low-level viremia. AIDS **24**:2405–2408.
19. **Ferrari G, et al.** 2011. Relationship between functional profile of HIV-1 specific CD8 T cells and epitope variability with the selection of escape mutants in acute HIV-1 infection. PLoS Pathog. **7**:e1001273. doi:10.1371/journal.ppat.1001273.
20. **Fiebig EW, et al.** 2003. Dynamics of HIV viremia and antibody seroconversion in plasma donors: implications for diagnosis and staging of primary HIV infection. AIDS **17**:1871–1879.
21. **Friedrich TC, et al.** 2007. Subdominant CD8+ T-cell responses are involved in durable control of AIDS virus replication. J. Virol. **81**:3465–3476.
22. **Gao X, et al.** 2005. AIDS restriction HLA allotypes target distinct intervals of HIV-1 pathogenesis. Nat. Med. **11**:1290–1292.
23. **Goonetilleke N, et al.** 2009. The first T cell response to transmitted/founder virus contributes to the control of acute viremia in HIV-1 infection. J. Exp. Med. **206**:1253–1272.

24. **Goudsmit J, et al.** 2002. Naturally HIV-1 seroconverters with lowest viral load have best prognosis, but in time lose control of viraemia. AIDS **16**: 791–793.
25. **Goulder PJ, et al.** 2001. Substantial differences in specificity of HIV-specific cytotoxic T cells in acute and chronic HIV infection. J. Exp. Med. **193**:181–194.
26. **Goulder PJ, et al.** 1996. Novel, cross-restricted, conserved, and immunodominant cytotoxic T lymphocyte epitopes in slow progressors in HIV type 1 infection. AIDS Res. Hum. Retrovir. **12**:1691–1698.
27. **Grenfell BT, et al.** 2004. Unifying the epidemiological and evolutionary dynamics of pathogens. Science **303**:327–332.
28. **Guindon S, Gascuel O.** 2003. A simple, fast, and accurate algorithm to estimate large phylogenies by maximum likelihood. Syst. Biol. **52**:696–704.
29. **Hecht FM, et al.** 2002. Use of laboratory tests and clinical symptoms for identification of primary HIV infection. AIDS **16**:1119–1129.
30. **Hecht FM, et al.** 2011. Identifying the early post-HIV antibody seroconversion period. J. Infect. Dis. **204**:526–533.
31. **Huson DH, Bryant D.** 2006. Application of phylogenetic networks in evolutionary studies. Mol. Biol. Evol. **23**:254–267.
32. **Karlsson AC, et al.** 2007. Sequential broadening of CTL responses in early HIV-1 infection is associated with viral escape. PLoS One **2**:e225. doi:10.1371/journal.pone.0000225.
33. **Kearney M, et al.** 2008. Frequent polymorphism at drug resistance sites in HIV-1 protease and reverse transcriptase. AIDS **22**:497–501.
34. **Kimura M.** 1983. The neutral theory of molecular evolution. Cambridge University Press, Cambridge, MA.
35. **Lefrere JJ, et al.** 1997. Even individuals considered as long-term nonprogressors show biological signs of progression after 10 years of human immunodeficiency virus infection. Blood **90**:1133–1140.
36. **Lemey P, et al.** 2007. Synonymous substitution rates predict HIV disease progression as a result of underlying replication dynamics. PLoS Comput. Biol. **3**:e29. doi:10.1371/journal.pcbi.0030029.
37. **Leslie A, et al.** 2005. Transmission and accumulation of CTL escape variants drive negative associations between HIV polymorphisms and HLA. J. Exp. Med. **201**:891–902.
38. **Leslie AJ, et al.** 2004. HIV evolution: CTL escape mutation and reversion after transmission. Nat. Med. **10**:282–289.
39. **Lindkvist A, et al.** 2009. Reduction of the HIV-1 reservoir in resting CD4+ T-lymphocytes by high dosage intravenous immunoglobulin treatment: a proof-of-concept study. AIDS Res. Ther. **6**:15.
40. **Lyles RH, et al.** 2000. Natural history of human immunodeficiency virus type 1 viremia after seroconversion and proximal to AIDS in a large cohort of homosexual men. Multicenter AIDS Cohort Study. J. Infect. Dis. **181**: 872–880.
41. **Makedonas G, et al.** 2009. Rapid up-regulation and granule-independent transport of perforin to the immunological synapse define a novel mechanism of antigen-specific CD8+ T cell cytotoxic activity. J. Immunol. **182**:5560–5569.
42. **Makedonas G, Betts MR.** 2011. Living in a house of cards: re-evaluating CD8+ T-cell immune correlates against HIV. Immunol. Rev. **239**:109–124.
43. **Makedonas G, et al.** 2010. Perforin and IL-2 upregulation define qualitative differences among highly functional virus-specific human CD8 T cells. PLoS Pathog. **6**:e1000798.
44. **Martinez-Picado J, et al.** 2006. Fitness cost of escape mutations in p24 Gag in association with control of human immunodeficiency virus type 1. J. Virol. **80**:3617–3623.
45. **Mellors JW, et al.** 1997. Plasma viral load and CD4+ lymphocytes as prognostic markers of HIV-1 infection. Ann. Intern. Med. **126**:946–954.
46. **Mendoza D, et al.** 2012. HLA B*5701-positive long-term nonprogressors/elite controllers are not distinguished from progressors by the clonal composition of HIV-specific CD8+ T cells. J. Virol. **86**:4014–4018.
47. **Migueles SA, Connors M.** 2001. Frequency and function of HIV-specific CD8(+) T cells. Immunol. Lett. **79**:141–150.
48. **Migueles SA, Connors M.** 2010. Long-term nonprogressive disease among untreated HIV-infected individuals: clinical implications of understanding immune control of HIV. JAMA **304**:194–201.
49. **Migueles SA, et al.** 2003. The differential ability of HLA B*5701+ long-term nonprogressors and progressors to restrict human immunodeficiency virus replication is not caused by loss of recognition of autologous viral gag sequences. J. Virol. **77**:6889–6898.
50. **Migueles SA, et al.** 2002. HIV-specific CD8+ T cell proliferation is coupled to perforin expression and is maintained in nonprogressors. Nat. Immunol. **3**:1061–1068.
51. **Migueles SA, et al.** 2008. Lytic granule loading of CD8+ T cells is required for HIV-infected cell elimination associated with immune control. Immunity **29**:1009–1021.
52. **Migueles SA, et al.** 2000. HLA B*5701 is highly associated with restriction of virus replication in a subgroup of HIV-infected long term nonprogressors. Proc. Natl. Acad. Sci. U. S. A. **97**:2709–2714.
53. **Miura T, et al.** 2009. HLA-B57/B*5801 human immunodeficiency virus type 1 elite controllers select for rare gag variants associated with reduced viral replication capacity and strong cytotoxic T-lymphocyte recognition. J. Virol. **83**:2743–2755.
54. **Munoz A, et al.** 1995. Long-term survivors with HIV-1 infection: incubation period and longitudinal patterns of CD4+ lymphocytes. J. Acquir. Immune Defic. Syndr. Hum. Retrovirol. **8**:496–505.
55. **Navis M, et al.** 2007. Viral replication capacity as a correlate of HLA B57/B5801-associated nonprogressive HIV-1 infection. J. Immunol. **179**: 3133–3143.
56. **Nei M, Gojobori T.** 1986. Simple methods for estimating the numbers of synonymous and nonsynonymous nucleotide substitutions. Mol. Biol. Evol. **3**:418–426.
57. **Nielsen R, Yang Z.** 1998. Likelihood models for detecting positively selected amino acid sites and applications to the HIV-1 envelope gene. Genetics **148**:929–936.
58. **O'Brien TR, et al.** 1996. Serum HIV-1 RNA levels and time to development of AIDS in the Multicenter Hemophilia Cohort Study. JAMA **276**: 105–110.
59. **O'Connell KA, et al.** 2010. Control of HIV-1 in elite suppressors despite ongoing replication and evolution in plasma virus. J. Virol. **84**:7018–7028.
60. **Palmer S, et al.** 2005. Multiple, linked human immunodeficiency virus type 1 drug resistance mutations in treatment-experienced patients are missed by standard genotype analysis. J. Clin. Microbiol. **43**:406–413.
61. **Pantaleo G, et al.** 1995. Studies in subjects with long-term nonprogressive human immunodeficiency virus infection. N. Engl. J. Med. **332**:209–216.
62. **Pereyra F, et al.** 2010. The major genetic determinants of HIV-1 control affect HLA class I peptide presentation. Science **330**:1551–1557.
63. **Peters HO, et al.** 2008. An integrative bioinformatic approach for studying escape mutations in human immunodeficiency virus type 1 gag in the Pumwani Sex Worker Cohort. J. Virol. **82**:1980–1992.
64. **Riou C, et al.** 2012. Distinct kinetics of Gag-specific CD4+ and CD8+ T cell responses during acute HIV-1 infection. J. Immunol. **188**:2198–2206.
65. **Rodes B, et al.** 2004. Differences in disease progression in a cohort of long-term non-progressors after more than 16 years of HIV-1 infection. AIDS **18**:1109–1116.
66. **Roederer M, Nozzi JL, Nason MC.** 2011. SPICE: exploration and analysis of post-cytometric complex multivariate datasets. Cytometry A **79**:167–174.
67. **Salemi M, et al.** 2007. Phylodynamics of HIV-1 in lymphoid and non-lymphoid tissues reveals a central role for the thymus in emergence of CXCR4-using quasispecies. PLoS One **2**:e950. doi:10.1371/journal.pone.0000950.
68. **Salemi M, Gray RR, Goodenow MM.** 2008. An exploratory algorithm to identify intra-host recombinant viral sequences. Mol. Phylogenet. Evol. **49**:618–628.
69. **Schmidt HA, Strimmer K, Vingron M, von Haeseler A.** 2002. TREE-PUZZLE: maximum likelihood phylogenetic analysis using quartets and parallel computing. Bioinformatics **18**:502–504.
70. **Sheppard HW, Lang W, Ascher MS, Vittinghoff E, Winkelstein W.** 1993. The characterization of non-progressors: long-term HIV-1 infection with stable CD4+ T-cell levels. AIDS **7**:1159–1166.
71. **Strimmer K, von Haeseler A.** 1997. Likelihood-mapping: a simple method to visualize phylogenetic content of a sequence alignment. Proc. Natl. Acad. Sci. U. S. A. **94**:6815–6819.
72. **Swanson WJ, Nielsen R, Yang Q.** 2003. Pervasive adaptive evolution in mammalian fertilization proteins. Mol. Biol. Evol. **20**:18–20.
73. **Swofford DL, Sullivan J.** 2009. Phylogeny inference based on parsimony and other methods using PAUP*, p 289–312. *In* Lemey P, Salemi M, Vandamme A-M (ed), The phylogenetic handbook: a practical approach to phylogenetic analysis and hypothesis testing. Cambridge University Press, Cambridge, MA.
74. **Tamura K, et al.** 2011. MEGA5: molecular evolutionary genetics analysis using maximum likelihood, evolutionary distance, and maximum parsimony methods. Mol. Biol. Evol. **28**:2731–2739.
75. **Tang Y, et al.** 2010. Correlates of spontaneous viral control among long-term survivors of perinatal HIV-1 infection expressing human leukocyte antigen-B57. AIDS **24**:1425–1435.

76. **Troyer RM, et al.** 2009. Variable fitness impact of HIV-1 escape mutations to cytotoxic T lymphocyte (CTL) response. PLoS Pathog. **5**:e1000365. doi:10.1371/journal.ppat.1000365.
77. **Wong WS, Yang Z, Goldman N, Nielsen R.** 2004. Accuracy and power of statistical methods for detecting adaptive evolution in protein coding sequences and for identifying positively selected sites. Genetics **168**:1041–1051.
78. **Yang Z.** 2000. Maximum likelihood estimation on large phylogenies and analysis of adaptive evolution in human influenza virus A. J. Mol. Evol. **51**:423–432.
79. **Yang Z.** 2007. PAML 4: phylogenetic analysis by maximum likelihood. Mol. Biol. Evol. **24**:1586–1591.
80. **Zimmerli SC, et al.** 2005. HIV-1-specific IFN-gamma/IL-2-secreting CD8 T cells support CD4-independent proliferation of HIV-1-specific CD8 T cells. Proc. Natl. Acad. Sci. U. S. A. **102**:7239–7244.